NANOPOROUS CARBON

***Lorentz JÄNTSCHI*[1], *Sorana D. BOLBOACĂ*[2]**

[1] Technical University of Cluj-Napoca
[2] Iuliu Hațieganu University of Medicine and Pharmacy Cluj-Napoca

DEFINITION

Nanoporous carbon is a form of carbon processed to have pores producing a high ratio between the available surface area and the volume. The size of the pores depends on the method used for preparation and are classified (Sing et al. 1985[1]) in micropores (<2 nm), mesopores (2-50 nm) and macropores (>50 nm). The term nanopore embraces the above three categories of pores, with an upper limit of 100 nm (Thommes et al. 2015[2]).

KEYWORDS:

Porous carbon; Activated carbon; Nanocarbon; Carbon aerogels

HISTORICAL ORIGIN(S)

Nanoporous carbon is a form of carbon processed to have pores producing a high ratio between the available surface area and the volume. Going back to its ancestors (activated charcoal; activated carbon), porous carbons are the oldest adsorbents known, the use of it being described in Egypt in 1550 BC (Cooney 1980[3]). In Europe, historical origin of activated carbon uses dates before 1900 (Wrench 1931[4]), its primary use being in the purification of drug and pharmaceutical products, while the first industrial production of activated carbons in US started in 1913 (Baker et al. 1992[5]). Systematic studies of nanoporous carbons (nPorC) began shortly after (Debye & Scherrer 1917[6]).

NANO-SCIENTIFIC DEVELOPMENT(S)

Today, nPorC can be prepared from organic natural (wood, nutshells, peat, lignite, coal, petroleum coke) and synthetic (polyacrylonitrile, polyvinylidene chloride, polyvinyl chloride, polyfurfuryl alcohol) and inorganic (metallic carbides) precursors while the pre-treatment of the natural precursors generally involves a reaction with a chemical reagent. The activation generally involves a thermal decomposition in inert or oxidative atmosphere, while for metallic carbides the removal of reaction wastes is conducted with a hydrogenation. These processes may be combined in different successions (see Figure 1) for archiving a specific purpose, which is generally driven by the size and the distribution of the pores.

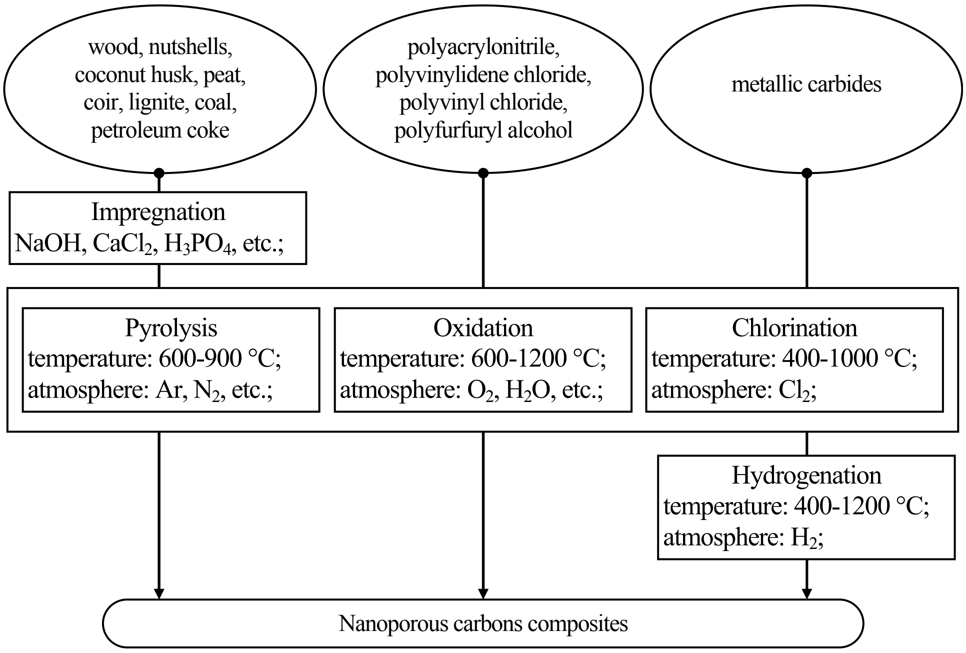

Figure 1. From carbon based materials to nPorC

The macrostructure of the nPorC can be templated (for instance with a mesoporous silica template) when the outcome (nPorC) is obtained after a supplementary step (of washing with a solvent) for removing the template (for an example please see Jong et al. 2002[7]). Auxiliary steps, such as short (15-90 minutes) treatment with NH_3 at 400-700 °C temperature may be involved having as purpose the increasing of the specific activated surface (as suggested in Gogotsi et al. 2006[8]).

When one desires controlled pore size and distribution, then the using of and/or starting from templates are the alternatives, when also the tuneable parameters includes a proper selection of the oxidative gas. Thus, following the procedure proposed in (Barsoum & Gogotsi 2004[9]), as heavier the halogen is used (F_2, Cl_2, Br_2, I_2), the larger resulted pores is obtained.

Carbon aerogels, belonging to nPorC, with a very low density (ranging in [0.035, 0.1] g/cm^3) can be obtained from organic aerogels (for different routes of organic aerogels preparation please see Pekala 1989[10]; Pekala et al. 1995[11]; Biesmans et al. 1998[12]; Li & Guo 2000[13]; Zhang et al. 2003[14]) by following a recipe similar with the one given in Figure 1, where the thermal decomposition is conducted with N_2 at 900°C in (Czakkelet al. 2005[15]), and in CO_2 at 950 °C in (Kabbour et al. 2006[16]). It has porosity over 50%, with pore diameter under 100 nm and surface areas ranging in [400, 1000] m^2/g.

The thermal treatment plays the essential role in the producing of the nPorC. Following table (see Table 1) adapted from (Mohun 1959[17]) provides a terminology of the outcome.

Table 1. Thermal treatment of materials to obtain nPorC

Temperature range	Outcome
600-700 °C	'chars', condensed molecular
700-1000 °C	'cokes', substantial amounts of carbon in disorganised phase
1000-2000 °C	'baked' carbons
2000-2500 °C	partially graphitized
> 2500 °C	polycrystalline graphite

NANO-CHEMICAL APPLICATION(S)

The development of nPorC materials are driven by their uses and vice versa. Their applications include:

- Filtering purposes, such as are separation, purification and barriers
    - In (Gilbert et al. 1982[18]) nPorC for gas chromatography and high-performance liquid chromatography is produced by impregnating a suitable silica gel or porous glass with a phenolformaldehyde resin mixture. After polymerisation within the pores of the template material the polymer is converted to glassy carbon by heating in an inert atmosphere to about 1000 °C. The silica template is then removed by alkali to and finally the material is fired in an inert atmosphere at a high temperature in the range 2000-2800 °C to anneal the surface, remove micropores and, depending upon the temperature, produce some degree of graphitization. In (Corbin et al. 2001[19]) nPorC with additives including TiO_2, SiO_2 and ethylene glycol synthesized by pyrolysis of one or more layers of polymer containing materials, wherein at least one of the pyrolyzed layers is a polymer and additive mixture, on a porous substrate so as to produce a thin mixed matrix film with pores for the separation of small molecules. In (Ribeiro et al. 2008[20]) are provided adsorption equilibrium data of CO_2, CH_4, and N_2 at 299 K to 423 K temperature and 0 kPa to 700 kPa pressure.
- For storage such as are electricity storage and matter storage
    - Energy storage. In (Oh et al. 2000[21]) is described a method of producing nPorC materials with pore sizes from 2 nm to 20 nm, in (Ruffordet al. 2009[22]) a method of reacting waste coffee grounds (or sugar cane bagasse) with an activating agent in an environment including at least one inert gas, in (Malentin et al. 2012[23]) includes additional doping the surface of the pores with nitrogen atoms (>10% N_2).
    - Fluids storage. In (Dimeo et al. 2008[24]) is describes the producing of nPorC composite having an average pore diameter of less than 10 nm, and when nPorC incorporates boron provides a hydrogen storage medium otherwise the use is as a chlorine storage medium (when according to the claims, the actual capacity of the porous carbon exceeds the capacity of the high-pressure liquid containment volume by approximately 30%). Also, according to same claims, in addition to chlorine, the approach may be applied to other industrial gases. In (Carruthers et al. 2011[25]) is described a nPorC prepared for fluid storage, dispensing and desulfurization (claiming a fill density >400 g/l, measured in gAsH_3 at 25°C and 650 mmHg per litter nPorC, or >30% pores sizes in [0.3-0.72] nm and >20% micropores < 2 nm or been formed by pyrolysis and optional activation, and having density of from 0.80 g/cm^3 to 2.0 g/cm^3.
    - Solid-like storage. In (Ting et al. 2015[26]) is reported confinement of molecular hydrogen in nPorC with characteristics commensurate with solid H_2 at temperatures up to 67 K above the liquid-vapor critical temperature of bulk H_2 occurring at 0.02 MPa pressure.
- For transformations such as are as actuator
    - In (Biener et al. 2010[27]) an actuator is designed to include an nPorC aerogel exhibiting charge-induced reversible strain, when nPorC is used as an electrode immersed in an electrolyte. When a small voltage relative to a reference electrode is applied to the nPorC an actuation appears.
- For catalyse such as are the one prospected in (Yu et al. 2010[28]), reviewed in (Su et al. 2013[29]), and prospected in (Qi & Su 2014[30]).
- For transport, such as of condensed hydrocarbons (Falk et al. 2015[31]).

Uses of nPorC of continuing importance include catalysis (Sharma 1991[32]), gas masks

(Bakajin et al. 2011[33]) and water treatment (Torad et al. 2014[34]), capture of volatile organic compounds (Dziura et al. 2014[35]) as well as newer includes fuel cell electrodes (Ji et al. 2010[36]), environmental remediation (Chartier et al. 2014[37]), rechargeable batteries (Zhao et al. 2015[38]), H_2 (Jae et al. 2012[39]) and CH_4 (Choi et al. 2016[40]) storage, and controlled drug delivery (Saha et al. 2015[41]).

MULTI-/TRANS- DISCIPLINARY CONNECTION(S)

Along with its use as reinforcements for composites, where the content of NanoC is below 5%, and where the integrated performances are based on the matrix materials (Ajayan & Tour 2007[42]).

Assembling NanoC into macroscopic superstructures is a strategy to devise multifunctional materials (for further details see Shimoda et al. 2002[43], Zhou et al. 2002[44], Lee et al. 2011[45], and Wu et al. 2012[46]).

On one hand, zeolites are another group of porous structures and on the other hand, are used as templates to provide nPorC. Four zeolites with large cages are given in the next table (see Table 2).

Table 2. Zeolites with large pores

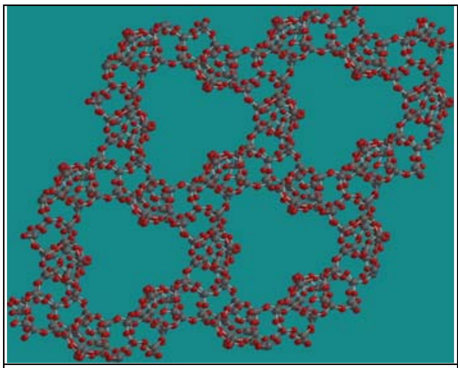	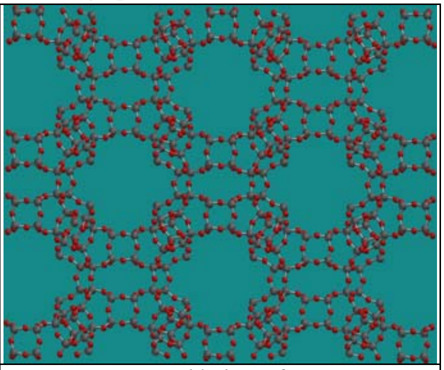
EWT with rings of 21 also with rings of 10, 6, 5, and 4	IFU with rings of 20 also with rings of 14, 12, 8, 6, 5, and 4
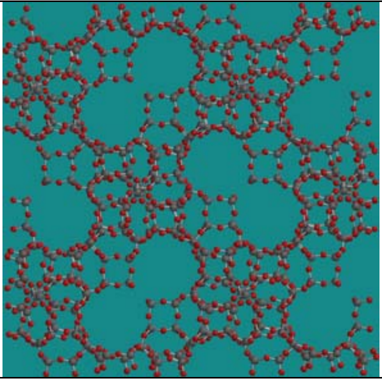	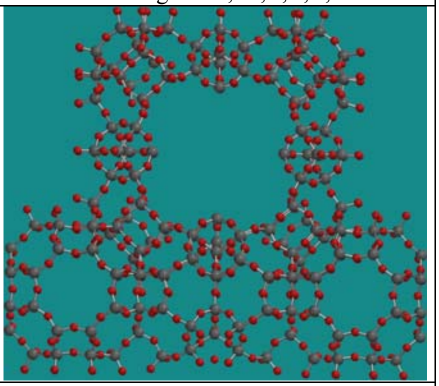
ITV with rings of 20 also with rings of 6 and 4	CLO with rings of 20 also with rings of 8, 6, and 4
For this and other zeolites please see http://izasc.ethz.ch/fmi/xsl/IZA-SC/ft.xsl	

It is difficult to evaluate the specific surface area of nPorC (see Stoeckli 1990[47]). A series of measurement and estimation strategies were designed including:

÷ Particle size distribution from diffraction. Laser diffraction spectroscopy (monochromatic light from a He-Ne laser can be used) uses the diffraction patterns (Fraunhofer diffraction equation, see Stewart & Korff 1928[48]) of the laser beam to measure geometrical dimensions of particles (see Figure 1). Particles of a given size diffract light through a given angle increasing with decreasing size (see McCave et al. 1986[49]).

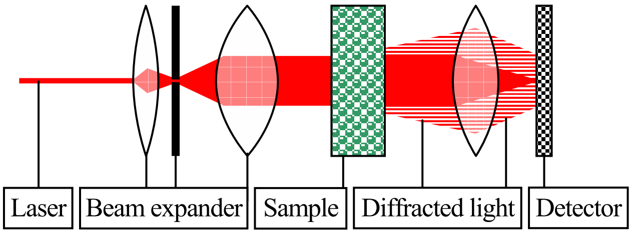

Figure 1. Particle size distribution from diffraction analysis

÷ Specific surface area estimated from experimental measurements. The specific surface area can be estimated from experimental measurements using different levels of theory (see Table 3).

Table 3. Monolayer and multilayer site binding models

Model	Langmuir	Brunauer-Emmett-Teller
Labels	p_A: partial pressure of adsorbate A; $[S]_0$, $[S]$, $[AS]$: concentrations of all (initial), free, and occupied sites; k_1, k_{-1}, K_{eq}: rate and equilibrium constants;	$[A_iS]$ concentration of the sites with i layers of A; p, p_0: equilibrium and saturation pressures of A; v, v_m: absorbed A total and monolayer volumes; E_1, E_L: heats for 1st layer and liquefaction;
Derive	$A_{(g)} + S_{(s)} \rightleftharpoons AS_{(s)}$ $k_1p_A[S] = v_1 = v_{-1} = k_{-1}[AS] \rightarrow K_{eq}p_A[S] = [AS]$ $[S]_0 = [S] + [AS] \rightarrow [AS]/[S]_0 = K_{eq}p_A/(1 + K_{eq}p_A)$ Rearranging, $p_A/[AS] = [S]_0^{-1}p_A + [S]_0^{-1}K_{eq}^{-1}$	$A_{(g)} + A_{i-1}S_{(s)} \rightleftharpoons A_iS_{(s)}$ $k_ip_A[A_{i-1}S] = v_{i-1} = v_{-i} = k_{-i}[A_iS]$ $k_1 = \exp(-E_1/RT)$, $k_i = \exp(-E_L/RT)$ $c = \exp(E_1/RT-E_L/RT)$ $(p_0/p-1)^{-1}v^{-1} = (v_m^{-1}-v_m^{-1}c^{-1})p/p_0 + v_m^{-1}c^{-1}$
Plots	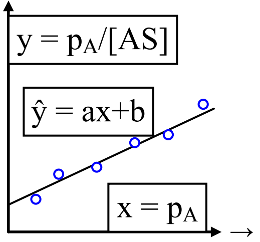 $\rightarrow [S]_0 = a^{-1}$ $K_{eq} = a/b$	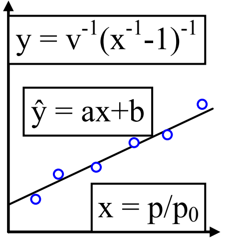 $v_m = (a+b)^{-1}$ $\rightarrow c = 1 + a/b$
SSA	$A_{Langmuir} = [S]_0 \cdot N_A \cdot s/m(S)$	$A_{total} = v_m \cdot N_A \cdot s/V_0(A)$; $A_{BET} = A_{total}/m(S)$
	Specific surface area (A_{Lng} or A_{BET}): accessible area of solid surface per unit mass of material s = cross section (occupied surface area) of one molecule of adsorbate; m(S) = mass of adsorbent; $N_A = 6.023 \cdot 10^{23}$ mol^{-1}; $V_0(A)$: molar volume of A;	

Extending Langmuir theory (Langmuir 1918[50]) for monolayer absorption to multilayer absorption, the Brunauer-Emmett-Teller theory (or BET, see Brunauer et al. 1938[51]) assumes (1) gas molecules physically adsorb on a solid in layers infinitely; (2) there is no interaction between each adsorption layer; and (3) the Langmuir theory can be applied to each layer (see Table 3). A modified BET technique has been adopted as ISO-9277:2010 (ISO 2010[52]) and as ASTM-D6556-14 (ASTM, 2014[53]).

÷ Qualitative surface analysis with microscopy. Scanning electron microscopy (see Figure 2) is involved for porosity visualization (see for instance Liu et al. 2016[54]).

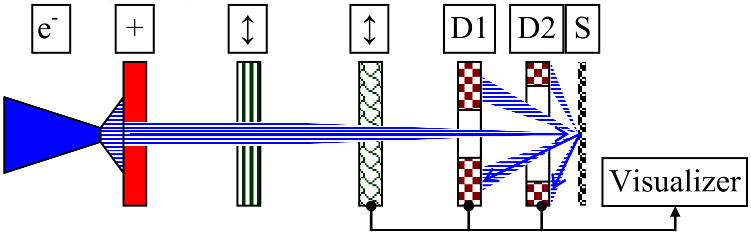

Figure 2. Porosity visualization with scanning electron microscopy

- Profiling from X-ray scattering (see Figure 3). Small angle X-ray scattering brings information about phenomena impacting large distance range such as pore filling, and wide angle X-ray scattering is used to study short (interatomic) distances (Trognko et al. 2015[55]).

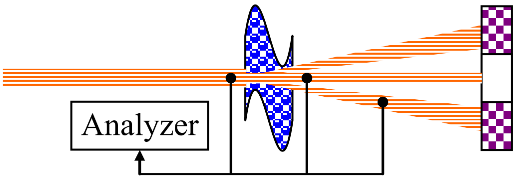

Figure 3. X-ray scattering for profiling

- Mercury's porosimetry and liquid nitrogen physisorption. Within a vacuum, mercury is intruded at high pressure into the sample (by using a porosimeter, see Figure 4). The pore size is determined based on the external pressure needed to force the liquid into the sample (Abell et al. 1999[56]). Similar experimental device is used for liquid N_2 absorption at -196°C (Oschatz 2014[57]). Derived parameters includes total pore surface area, pore size distribution, and total pore volume.

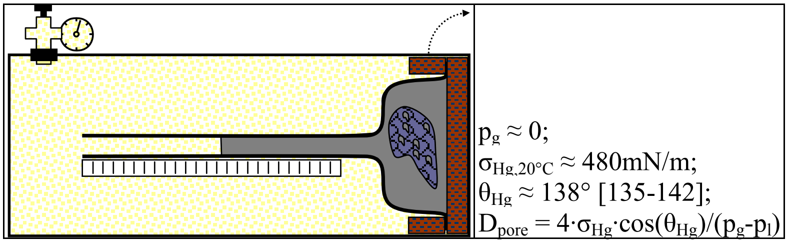

Figure 4. Porosimetry from mercury absorption

- Measurement of the heat of adsorption. Adsorption heat can be obtained from heating/cooling profile (see Figure 5) with an absorbed reference gas (such as n-butane, see Wollmann et al. 2012[58]) into the pores. The specific surface area can be retrieved after a calibration with reference materials (Wollmann et al. 2011[59]).

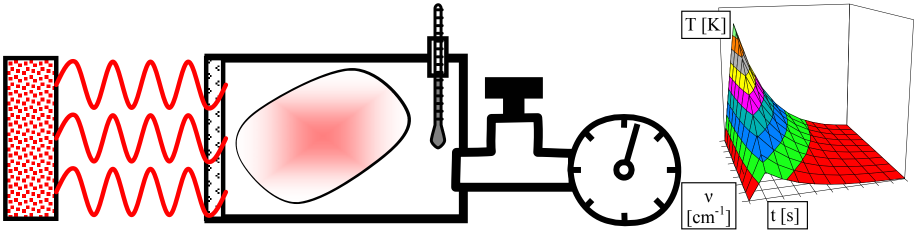

Figure 5. Porosimetry from thermal measurements

OPEN ISSUES

A series of models were designed to estimate the absorption space, specific surface area as well as the pore sizes distribution. For further details please see (Emmett 1948[60]), (Dubinin 1960[61]) and (Biggs & Buts 2006[62]).

RELATED LIST OF ABBREVIATIONS

So-called nanocarbons refer graphitic materials with at least one dimension below 100 nm: fullerenes, nanodiamonds (diamonds with a size below 1 μm), nano-onions (onion like carbon), CNTs (carbon nanotubes, single walled - SWCNT and multi-walled - MWCNT), nanofoams, graphene, nanofibers, nanoribbons, etc. (see see Figure 6).

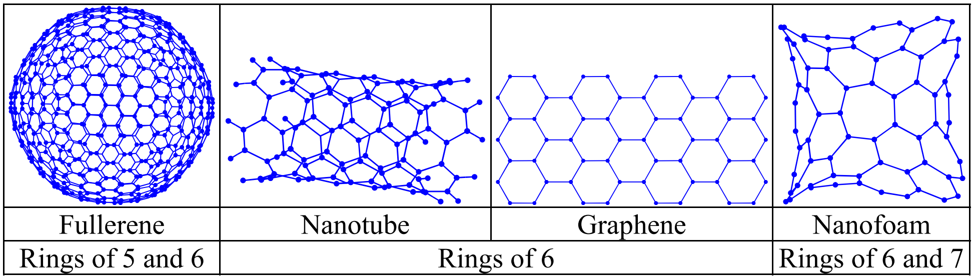

Figure 6. Nanocarbons

REFERENCES AND FURTHER READING

[1] Sing, K. S. W.; Everett, D. H.; Haul, R. A. W.; Moscou, L.; Pieroti, R. A.; Rouquerol, J.; Siemieniewska, T.; 1985. Reporting physisorption data for gas/solid systems with special reference to the determination of surface area and porosity (IUPAC Recommendations 1984). Pure and Applied Chemistry 57(4): 603-619.

[2] Thommes, M.; Kaneko, K.; Neimark, A. V.; Olivier, J. P.; Rodriguez-Reinoso, F.; Rouquerol, J.; Sing, K. S.W.; 2015. Physisorption of gases, with special reference to the evaluation of surface area and pore size distribution (IUPAC Technical Report). Pure and Applied Chemistry 87(9-10): 1051-1069.

[3] Cooney, O; 1980. Activated Charcoal: Antidotal and other Medical Uses. New York: M. Dekker.

[4] Wrench, J.; 1931. Origin, Properties and Uses of Activated Carbon. Oil & Fat Industries 8(12): 441-453.

[5] Baker, F.S.; Miller, C.E.; Repik, E.D.; 1992. Kirk-Othmer Encyclopedia of Chemical Technology. v. 4. New York: J. Wiley.

[6] Debye P.; Scherrer, P.; 1917. X-ray interference produced by irregularly oriented particles. III. Constitution of graphite and amorphous carbon. Physikalische Zeitschrift 18: 291-301.

[7] Jong, S. Y.; Jin G. L.; Seok C.; 2002. Method for preparing nanoporous carbons with enhanced mechanical strength and the nanoporous carbons prepared by the method. Patent US7326396 B2 from Feb. 5, 2008.

[8] Gogotsi, Y.; Yushin, G.; Hoffman, E. N.; Barsoum, M. M.; 2006. Process for producing nanoporous carbide derived carbon with large specific surface area. Patent WO2007062095 A1 from May 31, 2007.

[9] Barsoum, M. M.; Gogotsi, Y.; 2004. Nanoporous carbide derived carbon with tunable pore size. Patent WO2005007566 A3 from Jun. 30, 2005.

[10] Pekala, R. W.; 1989. Organic aerogels from the polycondensation of resorcinol with formaldehyde. Journal of materials science 24: 3221-3227.

[11] Pekala, R.W.; Alviso, C.T.; Lu, X.; Gross, J.; Fricke, J.; 1995. New organic aerogels based upon a phenolic-furfural reaction. Journal of Non-Crystalline Solids 188(1-2): 34-40.

[12] Biesmans, G.; Mertens, A.; Duffours, L.; Woignier, T.; Phalippou, J.; 1998. Polyurethane based organic aerogels and their transformation into carbon aerogels. Journal of Non-Crystalline Solids 225: 64-68.

[13] Li, W.C.; Guo, S.; 2000. Preparation of low-density carbon aerogels from a cresol/formaldehyde mixture. Carbon 38(10): 1520-1523.

[14] Zhang, R.; Li, W.; Liang, X.; Wu, G.; Lü, Y.; Zhan, L.; Lu, C.; Ling, L.; 2003. Effect of hydrophobic group in polymer matrix on porosity of organic and carbon aerogels from sol-gel polymerization of phenolic resole and methylolated melamine. Micropor. Mesopor. Mater. 62(1-2): 17-27.

[15] Czakkel, O.; Marthi, K.; Geissler, E.; Lászlo, K.; 2005. Influence of drying on the morphology of resorcinol-formaldehyde-based carbon gels. Microporous and Mesoporous Materials 86: 124-133.

---

[16] Kabbour, H.; Baumann, T.F.; Satcher, J. H. Jr.; Saulnier, A.; Ahn C. C.; 2006. Toward New Candidates for Hydrogen Storage: High-Surface-Area Carbon Aerogels. Chemistry of materials 18(26): 6085-6087.

[17] Mohun W. A.; 1959. Mineral active carbon and process for producing same. Patent US3066099 A from Nov. 27, 1962.

[18] Gilbert M. T.; Knox J. H.; Kaur B.; 1982. Porous glassy carbon, a new columns packing material for gas chromatography and high-performance liquid chromatography. Chromatographia 16: 138-146.

[19] Corbin, D. R.; Foley, H. C.; Shiflett, M. B.; 2001. Mixed matrix nanoporous carbon membranes. Patent EP1292380 A1 from Mar. 19, 2003.

[20] Ribeiro, R.P.; Sauer, T.P; Lopes, F.V.; Moreira, R.F.; Grande, C.A.; Rodrigues, A.E.; 2008. Adsorption of CO_2, CH_4, and N_2 in Activated Carbon Honeycomb Monolith. Journal of Chemical & Engineering Data 53(10): 2311-2317.

[21] Oh, S.-M.; Hyeon, T.-H.; Han, S.-J.; 2000. Method for preparing nanoporous carbon materials and electric double-layer capacitors using them. Patent US6515845 B1 from Feb. 4, 2003.

[22] Rufford, T. E.; Jurcakova, D.; Zhu Z.; Lu, G. Q.; 2009. Nanoporous carbon electrodes and supercapacitors formed therefrom. Patent WO2010020007 A1 from Feb. 25, 2010.

[23] Maletin, Y.; Stryzhakova N.; Zelinskyi S.; Gromadskyi D.; Tychyna S.; 2012. Method for selecting nanoporous carbon material for polarizable electrode, method for manufacturing such polarizable electrodes and method for manufacturing electrochemical double layer capacitor. Patent US2013139951 A1 from July 6, 2013.

[24] Dimeo, F. Jr.; Carruthers, J. D.; Wodjenski, M. J.; McManus, J. V.; Marzullo, J.; 2007. Nanoporous carbon materials, and systems and methods utilizing same. Patent WO2007136887 A2 from Jul. 24, 2008.

[25] Carruthers, J. D.; Dimeo, F. Jr.; Bobita, B.; 2011. Nanoporous articles and methods of making same. Patent US2011220518 A1 from Sept. 15, 2011.

[26] Ting, V.P.; Ramirez-Cuesta, A.J.; Bimbo, N.; Sharpe, J.E.; Noguera-Diaz, A.; Presser, V.; Rudic, S.; Mays T.J.; 2015. Direct Evidence for Solid-like Hydrogen in a Nanoporous Carbon Hydrogen Storage Material at Supercritical Temperatures. ACS Nano 9(8): 8249-8254.

[27] Biener J.; Baumann T. F.; Shao L.; Weissmueller J.; 2010. Nanoporous carbon actuator and methods of use thereof. Patent US2010230298 A1 from Sept. 16, 2010.

[28] Yu, D.; Nagelli, E.; Du, F.; Dai, L.; 2010. Metal-Free Carbon Nanomaterials Become More Active than Metal Catalysts and Last Longer. The Journal of Physical Chemistry Letters 1: 2165-2173.

[29] Su, D. S.; Perathoner, S.; Centi, G.; 2013. Nanocarbons for the Development of Advanced Catalysts. Chemical Reviews 113: 5782-5816.

[30] Qi, W.; Su, D.; 2014. Metal-Free Carbon Catalysts for Oxidative Dehydrogenation Reactions. ACS Catalysis 4: 3212-3218.

[31] Falk, K.; Coasne, B.; Pellenq, R.; Ulm, F.J.; Bocquet, L.; 2015. Subcontinuum mass transport of condensed hydrocarbons in nanoporous media. Nature Communications 6:6949(7p).

[32] Sharma, B.K.; 1991. Industrial chemistry (including chemical engineering). Meerut: Goel.

[33] Bakajin, O.; Holt, J.; Noy, A.; Park, H.G.; 2006. Membranes for nanometer-scale mass fast transport. Patent US8038887 B2 from Oct. 18, 2011.

[34] Torad, N. L.; Hu, M.; Ishihara, S.; Sukegawa, H.; Belik, A. A.; Imura, M.; Ariga, K.; Sakka, Y.; Yamauchi, Y.; 2014. Direct Synthesis of MOF-Derived Nanoporous Carbon with Magnetic Co Nanoparticles toward Efficient Water Treatment. Small 10: 2096-2107.

[35] Dziura, A.; Marszewski, M.; Choma, J.; Souza, L.K.C. de; Osuchowski, Ł.; Jaroniec, M.; 2014. Saran-Derived Carbons for CO_2 and Benzene Sorption at Ambient Conditions. Ind. Eng. Chem. Res. 53(40):15383-15388.

[36] Ji, X.; Lee, K.T.; Holden, R.; Zhang, L.; Zhang, J.; Botton, A.G.; Couillard, M.; Nazar L.F.; 2010. Nanocrystalline intermetallics on mesoporous carbon for direct formic acid fuel cell anodes. Nature Chemistry 2: 286-293.

[37] Chartier, Y.; Emmanuel, J.; Pieper, U.; Prüss, A.; Rushbrook, V.P.; Stringer, R.; Townend, W.; Wilburn, S.; Zghondi, R.; (Eds.) 2014. Safe management of wastes from health-care activities. Geneva: World Health Organization.

[38] Zhao, Q.; Lu, Y.; Zhu, Z.; Tao, Z.; Chen, J.; 2015. Rechargeable Lithium-Iodine Batteries with Iodine/Nanoporous Carbon Cathode. Nano Letters 15(9): 5982-5987.

---

[39] Yang, S.J.; Jung, H.; Kim, T.; Park, C.R.; 2012. Recent advances in hydrogen storage technologies based on nanoporous carbon materials. Progress in Natural Science: Materials International 22(6): 631-638.

[40] Choi, P.S.; Jeong, J.M.; Choi, Y.K.; Kim, M.S.; Shin, G.J.; Park, S.J.; 2016. A review: methane capture by nanoporous carbon materials for automobiles. Carbon Letters 17(1): 18-28.

[41] Saha, D.; Moken, T.; Chen, J.; Hensley, D.K.; Delaney, K.; Hunt, M.A.; Nelson, K.; Spurri, A.; Benham, L.; Brice, R.; Azoro, M.; 2015. Micro-/mesoporous carbons for controlled release of antipyrine and indomethacin. RSC Advances 5: 23699-23707.

[42] Ajayan, P. M.; Tour, J. M.; 2007. Nanotube Composites. Nature 447: 1066-1068.

[43] Shimoda, H.; Oh, S. J.; Geng, H. Z.; Walker, R. J.; Zhang, X. B.; McNeil, L. E.; Zhou, O.; 2002. Self-Assembly of Carbon Nanotubes. Adv. Mater. 14: 899-901.

[44] Zhou, O.; Shimoda, H.; Gao, B.; Oh, S.; Fleming, L.; Yue, G.; 2002. Materials Science of Carbon Nanotubes: Fabrication, Integration, and Properties of Macroscopic Structures of Carbon Nanotubes. Acc. Chem. Res. 35: 1045-1053.

[45] Lee, S. H.; Lee, D. H.; Lee, W. J.; Kim, S. O.; 2011. Tailored Assembly of Carbon Nanotubes and Graphene. Adv. Funct. Mater. 21: 1338-1354.

[46] Wu, D.; Zhang, F.; Liang, H.; Feng, X.; 2012. Nanocomposites and Macroscopic Materials: Assembly of Chemically Modified Graphene Sheets. Chem. Soc. Rev. 41: 6160-6177.

[47] Stoeckli, H.F.; 1990. Microporous carbons and their characterization: The present state of the art. Carbon 28(1): 1-6.

[48] Stewart, J.Q.; Korff S.A.; 1928. The refractive index of sodium vapor and the width of the D lines in absorption. Physical review 32: 676-680.

[49] McCave, I.N.; Bryant, R.J.; Cook, H.F.; Coughanowr, C.A.; 1986. Evaluation of a laser-diffraction-size analyzer for use with natural sediments: research method paper. Journal of Sedimentary Petrology 56(4): 561-564.

[50] Langmuir, I.; 1918. The adsorption of gases on plane surfaces of glass, mica and platinum. Journal of the American Chemical Society 40(9): 1361-1403.

[51] Brunauer, S.; Emmett, P. H.; Teller, E.; 1938. Adsorption of Gases in Multimolecular Layers. Journal of the American Chemical Society 60 (2): 309-319.

[52] ISO; 2010. Determination of the specific surface area of solids by gas adsorption - BET method. ISO 9277:2010(E). Geneva: International Organization for Standardization.

[53] ASTM; 2014. Standard Test Method for Carbon Black - Total and External Surface Area by Nitrogen Adsorption. ASTM D6556 - 14. DOI: 10.1520/D6556-14.

[54] Liu, X.; Wang, C.; Wu, Q.; Wang Z.; 2016. Magnetic porous carbon-based solid-phase extraction of carbamates prior to HPLC analysis. Microchimica Acta 183(1): 415-421.

[55] Trognko, L.; Lecante, P.; Ratel-Ramond, N.; Rozier, P.; Daffos, B.; Taberna, P.-L.; Simon, P.; 2015. TiC-carbide derived carbon electrolyte adsorption study by ways of X-ray scattering analysis. Materials for Renewable and Sustainable Energy 4:17(6p).

[56] Abell, A.B.; Willis, K.L.; Lange D.A.; 1999. Mercury Intrusion Porosimetry and Image Analysis of Cement-Based Materials. Journal of Colloid and Interface Science 211: 39-44.

[57] Oschatz, M.; 2014. New routes towards nanoporous carbon materials for electrochemical energy storage and gas adsorption. PhD Thesis (PhD Advisor: Kaskel, S.), Technical University of Dresda.

[58] Wollmann, P.; Leistner, M.; Grählert, W.; Throl, O.; Dreisbach, F.; Kaskel, S. 2012. Infrasorb: Optical detection of the heat of adsorption for high throughput adsorption screening of porous solids. Microporous and Mesoporous Materials 149(1): 86-94.

[59] Wollmann, P.; Leistner, M.; Grählert, W.; Stoeck, U.; Grünker, R.; Gedrich, K.; Klein, N.; Throl, O.; Grählert, W.; Senkovska, I.; Dreisbach, F.; Kaskel, S. 2011. High-throughput screening: speeding up porous materials discovery. Chemical Communications 47(18): 86-94.

[60] Emmett, P.H.; 1948. Adsorption and pore-size measurements on charcoals and whetlerites. Chemical reviews 43(1): 69-148.

[61] Dubinin, M.M.; 1960. The potential theory of adsorption of gases and vapors for adsorbents with energetically nonuniform surfaces. Chemical reviews 60(2): 235-241.

[62] Biggs, M.J.; Buts, A.; 2006. Virtual porous carbons: What they are and what they can be used for. Molecular Simulation 32(7): 579-593.